^{7}Li and ^{7}Be DEEXCITATION LINES: PROBES FOR ACCELERATED PARTICLE TRANSPORT MODELS IN SOLAR FLARES

R. J. MURPHY
Universities Space Research Association
Naval Research Laboratory

X.-M. HUA
Institute for Space and Terrestrial Science
York University

B. KOZLOVSKY
Department of Physics and Astronomy
Tel Aviv University

R. RAMATY
Laboratory for High Energy Astrophysics
Goddard Space Flight Center

ABSTRACT

The photon energy spectrum of a spectral feature composed of the 429 and 478 keV gamma-ray lines from ^{7}Be and ^{7}Li (produced by interactions of flare-accelerated α particles with ambient He in the solar atmosphere) depends on the angular distribution of the interacting accelerated particles. We calculate this spectrum for limb and disc-centered flares using a loop model for the transport of the ions. In this model, the flux tube magnetic field is constant in the corona and converges in the chromosphere to the photosphere. Magnetic mirroring and MHD pitch-angle scattering are both taken into account. We compare the resulting spectra with data from the 1981 April 27 limb flare obtained with the gamma-ray spectrometer on SMM and provide convincing evidence for the existence of the ^{7}Li–^{7}Be feature in this flare. We show that data of this quality are adequate to distinguish between model spectra calculated for limb flares and spectra calculated for disc-centered flares. But the data are incapable of distinguishing limb-flare spectra derived with pitch-angle scattering from spectra derived without, since both provide good fits to these data. We show further that the data are also consistent with the spectrum derived for an isotropic distribution of interacting accelerated particles, but not with the spectrum derived for a beam normal to the line of sight, as would be a downward beam in a limb flare.

Subject Headings: gamma rays:general—hydromagnetics—Sun:flares

model for α particles. We then compare the results with data obtained with the gamma-ray spectrometer on SMM from the limb flare of 1981 April 27 (Forrest 1983) using the techniques developed by Murphy *et al.* (1985a,b) and Murphy (1985) for the comparison of theoretically-derived photon spectra with observed pulse-height spectra. We attempt to fit the data both with and without the ^{7}Li–^{7}Be feature. When the feature is not included, the fit is quite poor. However, fitting with spectra derived using the transport-model for limb flares results in a good fit, thus implying the production of ^{7}Li and ^{7}Be in solar flares. In addition to the transport-model spectra, we also consider ^{7}Li–^{7}Be spectra resulting from assumed angular distributions for the interacting α particles. We consider an isotropic angular distribution, a beam directed downward to the photosphere, and a perfect fan beam.

II. THE TRANSPORT MODEL AND THE RESULTANT PHOTON ENERGY SPECTRA

First, we briefly describe the transport model (for more details, see HRL; Miller and Ramaty 1989; Ramaty *et al.* 1989) and then present numerical results for the energy spectrum of the ^{7}Li–^{7}Be feature. The model consists of a single loop or a system of essentially identical loops. Each loop has a coronal segment, in which the magnitude of the magnetic field is constant, and two subcoronal segments in which the magnetic field and gas density increase with increasing depth. The subcoronal segments are parallel to a solar radius and extend from the ends of the coronal segment at the transition region into the chromosphere and photosphere. The magnetic field B in the subcoronal segments is assumed to vary as a power δ of the pressure. In the present paper we use $\delta = 0.2$ which, with the atmospheric model used by HRL, leads to an increase in B by about an order of magnitude from the transition region to the photosphere. It has been shown (Miller and Ramaty 1989) that this value of δ gives a reasonable fit to the angular distribution of the > 10 MeV bremsstrahlung suggested by the observed (Rieger *et al.* 1983; Rieger 1989) distribution of flare locations on

transit time through the loop, the coronal distribution becomes isotropic and there is no further decrease in the loss time. This regime of strong pitch-angle scattering is referred to as the saturated regime. At saturation, even though the coronal distribution is isotropic, the distribution in the subcoronal segments, where there is no pitch-angle scattering, remains anisotropic. The pitch-angle scattering rate can be expressed in terms of the scattering mean free path, Λ. HRL showed that saturation occurs when $\lambda \equiv \Lambda/L_c \simeq 25$, where L_c is the half-length of the coronal segment of the loop. HRL also showed that the decaying portions of the time profile of the 4.1—6.4 MeV nuclear line emission in the 1980 June 21 flare can be well fit with the instantaneous injection of protons at the top of a loop with $\delta = 0.2$ and a pitch-angle scattering rate close to saturation.

Using this transport model, we have evaluated the time-integrated angular distribution of the interacting α particles, weighted with the probability for producing gamma rays in the ^{7}Li–^{7}Be feature. This angular distribution is given by

$$\langle \frac{dN}{d\Omega} \rangle = \frac{\int dt \int dh \int dE\ v(E) N(E,h,\theta,t) n_{\rm He} \sigma(E)}{Q_\gamma}. \qquad (1)$$

Here t is time; h is height in the loop; E, v and θ are particle energy/nucleon, speed and pitch angle; $N(E,h,\theta,t)$ is the instantaneous differential α-particle number; $n_{\rm He}$ is the ambient He density; σ is the sum of the cross sections of the reactions ^{4}He$(\alpha,{\rm p})^7$Li* and ^{4}He$(\alpha,{\rm n})^7$Be*; Ω is the solid angle corresponding to the direction defined by θ; and Q_γ is the total gamma-ray yield in the ^{7}Li–^{7}Be feature. The integral of $\langle \frac{dN}{d\Omega} \rangle$ over Ω yields unity.

The results are shown in Figures 1 and 2 for $\lambda \rightarrow \infty$ and $\lambda = 20$, respectively. Here the angle θ is measured with respect to the direction of the magnetic field in the loop. As we pointed out, we take the magnetic field in the subcoronal segments to be parallel to a solar radius. If we further assume that the coronal magnetic field is also along the radial direction, then the field is parallel to a solar radius throughout the interaction region and θ can be measured with respect to

The resultant emissions, integrated over all photon energies, are given in Table 1 for various values of λ. Here $dQ_\gamma/d\Omega$ is the emission escaping from the solar atmosphere per unit solid angle around θ_{obs}, the angle between the direction of observation and an outward solar radius. For a flare at disc center, $\theta_{obs} = 0°$, while for a flare on the limb, $\theta_{obs} = 90°$. We also give in Table 1 the angle-averaged and energy-integrated photon production, $Q_\gamma/4\pi$, evaluated before the removal of the Compton scattered photons. The variation of Q_γ with λ is entirely due to Monte-Carlo statistics. The variation of $dQ_\gamma/d\Omega$ with λ and θ shows the effects of the angular dependence of the photon production and the removal of the photons by Compton scattering. We see that, in general, these effects are not very large. Nonetheless, the indicated variations are quite instructive. For both 0° and 45° there is very little Compton scattering and hence the decrease of the emission with decreasing λ is due to the angular dependence of the emission. As λ decreases, the interacting particles are more strongly downward peaked (compare Figures 1 and 2) and the emission in the upward direction is therefore reduced. The difference between the angle-averaged production and the escaping emission at both 0° and 45°, as well as the increase of $dQ_\gamma/d\Omega$ from $\theta = 0°$ to 45° for a fixed λ, are also due to the angular dependence of the emission. However, for a given λ, the decrease in $dQ_\gamma/d\Omega$ from 45° to 90° is due to photon removal by Compton scattering. Furthermore, at 90° the decrease in the emission with decreasing λ is due mostly to Compton scattering.

By examining the values given in Table 1, we see that Compton scattering is important only if the flare is close to the limb and, then, only if the pitch-angle scattering is strong. For example, for $\cos\theta_{obs} = 0$ and $\lambda \to \infty$, as much as 95% of the photons escape without scattering. This is because magnetic mirroring prevents the particles from penetrating deep into the atmosphere so that, even for a limb flare, the amount of matter traversed by an escaping photon is not large enough to cause significant Compton scattering. However, when the pitch-angle scattering rate approaches saturation and the flare is on the limb, Compton scattering becomes quite important. We find that for $\lambda = 20$ and $\theta = 90°$, only

for an assumed downward beam of interacting α particles viewed at disc center (see their figure 2). But the distribution of interacting α particles for saturated pitch angle scattering is quite different from a unidirectional downward beam, as can be seen in Figure 2 where a downward beam would correspond to a spike at $\cos\theta = -1$. This difference leads to qualitatively different results when the flare is viewed on the limb. Whereas the spectrum for a unidirectional beam consists of two narrow lines at the rest energies of 429 and 478 keV (see MKR figure 3), the spectrum for the much broader distribution of Figure 2 is broadened into a single feature with a peak at $\sim$ 450 keV (Figure 6). This spectrum is further modified by the addition of the scattered photons (Figure 7).

III. COMPARISON WITH DATA

We use the above results to analyze the 1981 April 27 limb flare (located at W88N16) observed with the gamma-ray spectrometer on SMM (Forrest 1983). This flare produced the most detailed astrophysical gamma-ray spectrum yet observed. The flare began at about 08:04 UT and produced significant gamma-ray emission for more than 30 minutes. A background-subtracted spectrum was obtained over the energy range 0.3 to 8.5 MeV for the time interval 08:04:00.841 to 08:35:57.769 UT by subtracting from the observed time-integrated count spectrum the average of the spectra observed the day before and the day after the flare observation, adjusted for the flare-observation live time. The resulting solar flare spectrum contained a number of nuclear lines and was analyzed previously by Murphy *et al.* (1985a,b) and Murphy (1985) to determine the abundances of the ambient gas in the interaction region.

To compare the calculated ^{7}Li–^{7}Be spectra with these data, we have used the method developed for the abundance determination. In this method, the gamma-ray spectrum expected from a solar flare is modeled with 15 components: an electron bremsstrahlung continuum assumed to be a power law; a positron annihilation line at 511 keV with an accompanying orthopositronium continuum; a neutron capture line at 2.223 MeV; and individual gamma-ray

MeV) for this flare. We do not include the neutron capture spectrum since the 2.223 MeV line was very weak in this limb flare and, furthermore, contributes only a featureless, flat continuum in the energy range of interest here. This results in 5 fitted parameters: the 4 intensities of the 4 components plus the power-law index. For a particular ^{7}Li–^{7}Be feature, these parameters are varied to minimize χ^2. The resulting values of χ^2 can be compared to see which distribution provides the best fit.

The resulting best-fit spectra are shown in Figures 8 through 15. Figures 8 through 12 are for the five ^{7}Li–^{7}Be features given in Figures 3 through 7. Figure 13 is for an assumed isotropic distribution of interacting α particles, Figure 14 is for an assumed downward beam on the limb, and Figure 15 is for an assumed perfect fan beam on the limb. The photon spectra for the latter three cases are from MKR (see their figure 3). In Figure 16 we show a fit obtained by excluding the He spectrum. The data points shown in Figures 8 through 16 were obtained by subtracting the best-fit power law from the observations. The curves marked N, ^{7}Li–^{7}Be and e^+ represent the nuclear component, the He spectrum (which, in the energy range of interest, is dominated by the ^{7}Li–^{7}Be feature), and the annihilation radiation, respectively. Table 2 gives the qualities of fit for the nine models corresponding to Figures 8 through 16. The two different values of f for model 9 will be discussed below. In the table, d.o.f. denotes the degrees of freedom and P is the probability that a randomly-observed count spectrum generated by the given model could have produced a χ^2 as large or larger. A smaller P implies a less acceptable model.

Since the 1981 April 27 flare was very close to the solar limb, we would expect that models 2, 4 and 5 would give better fits than models 1 and 3. We see that this is indeed the case, as the values of P for the two disc-center models (0.293 and 0.178) are significantly lower than those of the 3 limb models (0.503, 0.513 and 0.478). Limb models 2, 4 and 5 provide good fits because they all produce a peak at $\sim$ 450 keV (see also Figures 4, 6 and 7) which is clearly present in

Considering model 6 for an assumed isotropic distribution (Figure 13), we see that the calculated spectrum fits the data very well. This is because the spectrum resulting from this model, with a peak at $\sim$ 450 keV, is quite similar to that from a loop model for a limb flare with saturated pitch-angle scattering (compare figure 3 in MKR with Figure 6 or 7). Therefore, it would probably be impossible to determine from observations of a limb flare whether the interacting α particles are isotropic or have an angular distribution such as predicted by the transport model with saturated pitch-angle scattering. But observations with a Ge detector could distinguish the isotropic model from the model with no pitch-angle scattering, as the line at $\sim$ 400 keV would be an indication for the latter (see Figure 4). On the other hand, for a flare close to disc center, the spectra produced by the transport model are qualitatively different from that produced by the isotropic model (compare Figures 3 and 5 with figure 2 in MKR) and hence could be distinguished with a Ge detector or perhaps even with a NaI detector.

For the assumed downward beam on the limb (model 7), the fit to the data is quite poor. This model produces a spectrum similar to that of the disc center model with no pitch-angle scattering (Figure 3). In both cases the interacting particle distribution peaks in a direction normal to the line of sight. As we have discussed above, such a spectrum fails to reproduce both the peak at $\sim$ 450 keV and the dip at $\sim$ 480 keV that are seen in the data (see Figure 14). That the downward-beamed distribution does not provide a good a fit is consistent with the conclusion of Hua and Lingenfelter (1987) who rejected the downward beam on the basis of neutron data. For an assumed perfect fan beam on the limb, the resulting spectrum is quite similar to the spectrum produced by the transport model with no pitch-angle scattering. The resultant fit (model 8 in Table 2) is very good (see Figure 15).

We finally turn to model 9 where we have removed the interactions with ambient He. We see in Figure 16 that the fit is very poor because the peak around 450

We have evaluated the photon energy spectrum of a nuclear deexcitation line feature resulting from interactions of accelerated α particles with ambient He in solar flares. This feature, the ^{7}Li–^{7}Be feature, is composed of a pair of lines at 429 and 478 keV resulting from deexcitations of ^{7}Be and ^{7}Li, respectively. Because of their large masses, the excited ^{7}Li and ^{7}Be nuclei move in essentially the same directions as the incoming α particles, leading to Doppler shifts as large as 8% (see MKR for further details). These shifts can be studied even with relatively low resolution NaI spectrometers such as the gamma-ray spectrometer on SMM.

We have used a recently-developed loop model for the transport of ions in solar flares (HRL) to calculate the expected spectrum of the ^{7}Li–^{7}Be feature. In this model, the magnetic field is perpendicular to the photosphere, the flux tubes are converging in the chromosphere, and magnetic mirroring and MHD pitch-angle scattering are taken into account. We found that the spectrum of the ^{7}Li–^{7}Be feature depends on the pitch-angle scattering rate as well as on the location of the flare on the solar disc.

We have compared the calculated spectra with data from the 1981 April 27 flare obtained with the gamma-ray spectrometer on SMM (Forrest 1983). This flare was located very close to the limb. The sensitivity of our technique is demonstrated by the fact that spectra calculated for limb flares fit the data much better than spectra derived assuming the flare is at disc center. We were, however, not able to differentiate between spectra obtained with or without pitch-angle scattering.

We also compared the data to previously-derived photon spectra (MKR) obtained from assumed angular distributions of interacting α particles. We showed that a downward beam of interacting particles can be ruled out. We also showed that the 1981 April 27 limb-flare data cannot be used to distinguish an isotropic distribution from any of the distributions predicted by the transport model for

Kozlovsky, B., and Ramaty, R. 1974, *Astrophys. J.*, **191**, L43.

Kozlovsky, B. and Ramaty, R. 1977, *Ap. Letters*, **19**, 19.

MacKinnon, A.L., and Brown, J.C. 1989, *Astron. Astrophys.*, in press.

Miller, J.A., and Ramaty, R. 1989, *Ap. J.*, in press.

Murphy, R. J. 1985, *Gamma Rays and Neutrons from Solar Flares*, Ph.D. Dissertation, University of Maryland.

Murphy, R.J., Dermer, C.D., and Ramaty, R. 1987, *Ap. J. Supp.*, **63**, 721.

Murphy, R. J., Forrest, D. J., Ramaty, R., and Kozlovsky, B. 1985b, *19th Internat. Cosmic Ray Conference Papers*, **4**, 253.

Murphy,R. J.,Kozlovsky, B., and Ramaty, R. 1988,*Ap. J.* **331**, 1029.

Murphy, R. J. and Ramaty, R. 1984, *Adv. Space Res.* **4**, No. 7, 127.

Murphy, R. J., Ramaty, R., Forrest, D. J., and Kozlovsky, B. 1985a, *19th Internat. Cosmic Ray Conference Papers*, **4**, 249.

Ramaty, R., Kozlovsky, B., and Lingenfelter, R. E. 1979, *Ap. J. Suppl.*, **40**, 487.

Ramaty, R., Miller, J.A., Hua, X.-M., and Lingenfelter, R.E. 1988, in *Nuclear Spectroscopy of Astrophysical Sources*, ed. N. Gehrels and G.H. Share (New York: AIP), p. 217.

Ramaty, R., Miller, J.A., Hua, X.-M., and Lingenfelter, R.E. 1989, *Ap. J. Suppl.*, submitted.

Rieger, E. 1989, *Solar Phys.*, in press.

Rieger, E., Reppin, C., Kanbach, G., Forrest, D.J., Chupp, E.L., and Share, G.H. 1983, *Proc. 18th Internat. Cosmic Ray Conf.*, **10**, 338.

FIGURE CAPTIONS

Fig. 1.—The angular distribution of the interacting α particles (see equation 1) in a magnetic loop model with magnetic field convergence parameter $\delta = 0.2$ as a function of the pitch angle θ. The accelerated α particles are released instantaneously at the top of the coronal portion of the loop, their energy spectrum is a Bessel function with $\alpha T = 0.02$, and they suffer no pitch-angle scattering in the corona.

Fig. 2.—Same as in Figure 1, except that there is strong pitch-angle scattering in the corona.

Fig. 3.—Energy spectrum of the ^{7}Li–^{7}Be feature for a flare observed at disc center. The parameters defining the distribution of the interacting α particles are the same as in Figure 1. Compton scattering is taken into account, but the spectrum consists of only those photons which are not scattered in the solar atmosphere.

Fig. 4.—Energy spectrum of the ^{7}Li–^{7}Be feature for a flare observed on the limb. The parameters defining the distribution of the interacting α particles are the same as in Figure 1. Compton scattering is taken into account, but the spectrum consists of only those photons which are not scattered in the solar atmosphere.

Fig. 5.—Energy spectrum of the ^{7}Li–^{7}Be feature for a flare observed at disc center. The parameters defining the distribution of the interacting α particles are the same as in Figure 2. Compton scattering is taken into account, but the spectrum consists of only those photons which are not scattered in the solar atmosphere.

Fig. 6.—Energy spectrum of the ^{7}Li–^{7}Be feature for a flare observed on the limb. The parameters defining the distribution of the interacting α particles are the same as in Figure 2. Compton scattering is taken into account, but the

Fig. 14.—Same as in Figure 8, except that the ^{7}Li–^{7}Be feature corresponds to a photon spectrum obtained by assuming that the interacting α particles form a downward beam and the flare is on the limb.

Fig. 15.—Same as in Figure 8, except that the ^{7}Li–^{7}Be feature corresponds to a photon spectrum obtained by assuming that the interacting α particles form a perfect fan and the flare is on the limb.

Fig. 16—Same as in Figure 8, but without the ^{7}Li–^{7}Be feature. As in Figures 8 through 15, the positronium fraction f = 0.67.

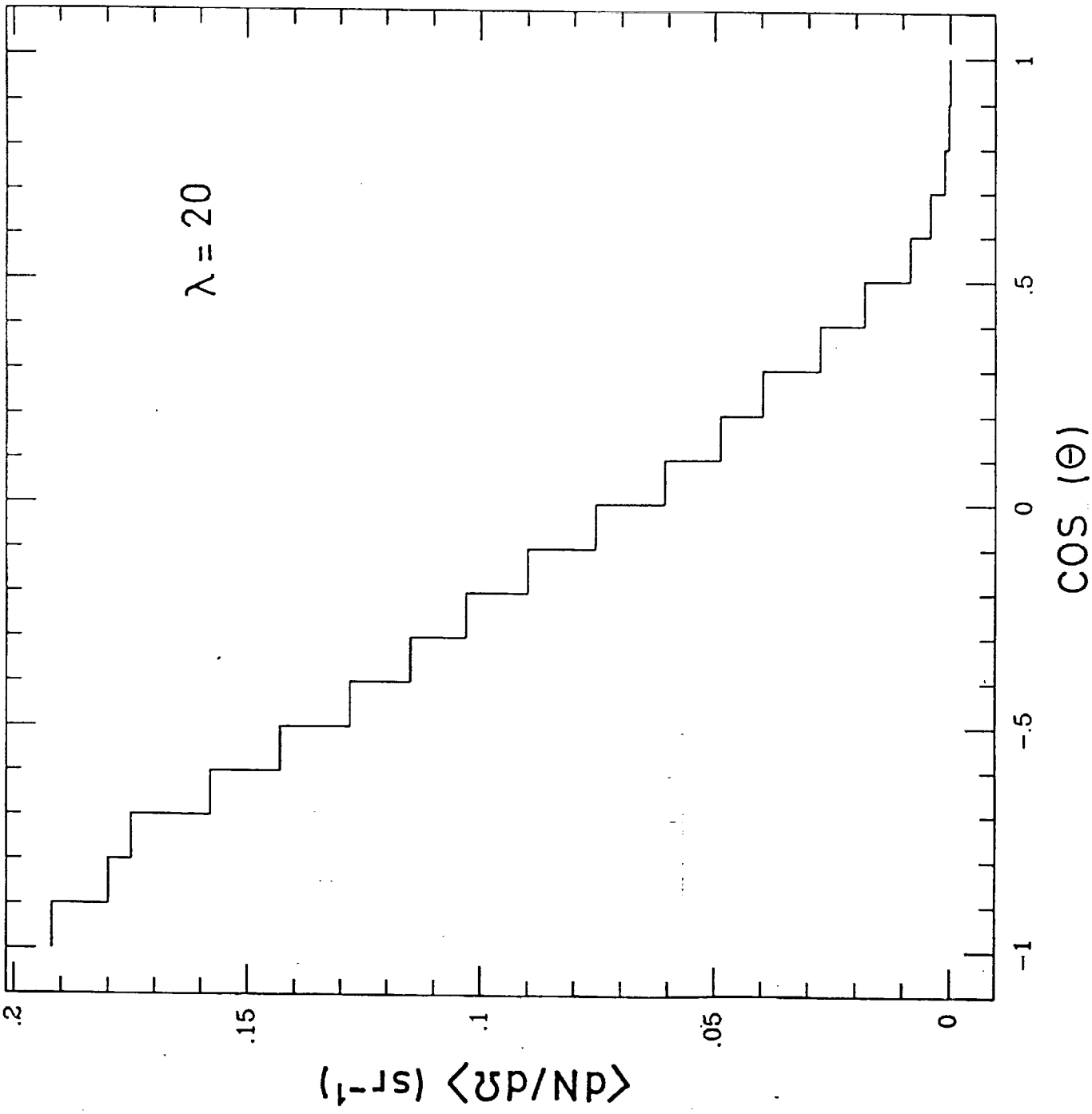

PRECEDING PAGE BLANK NOT FILMED

Figure 2

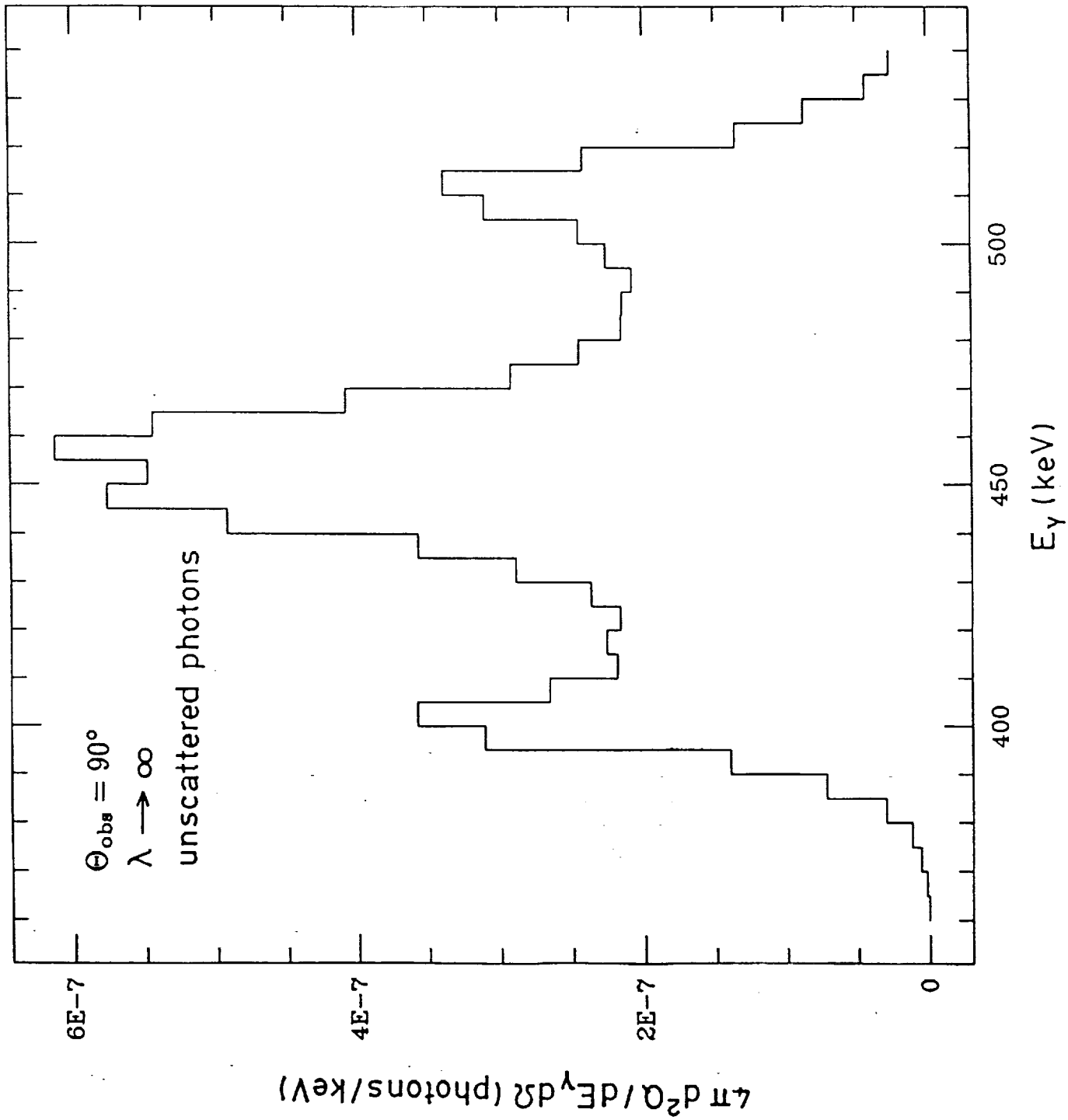

Figure 4

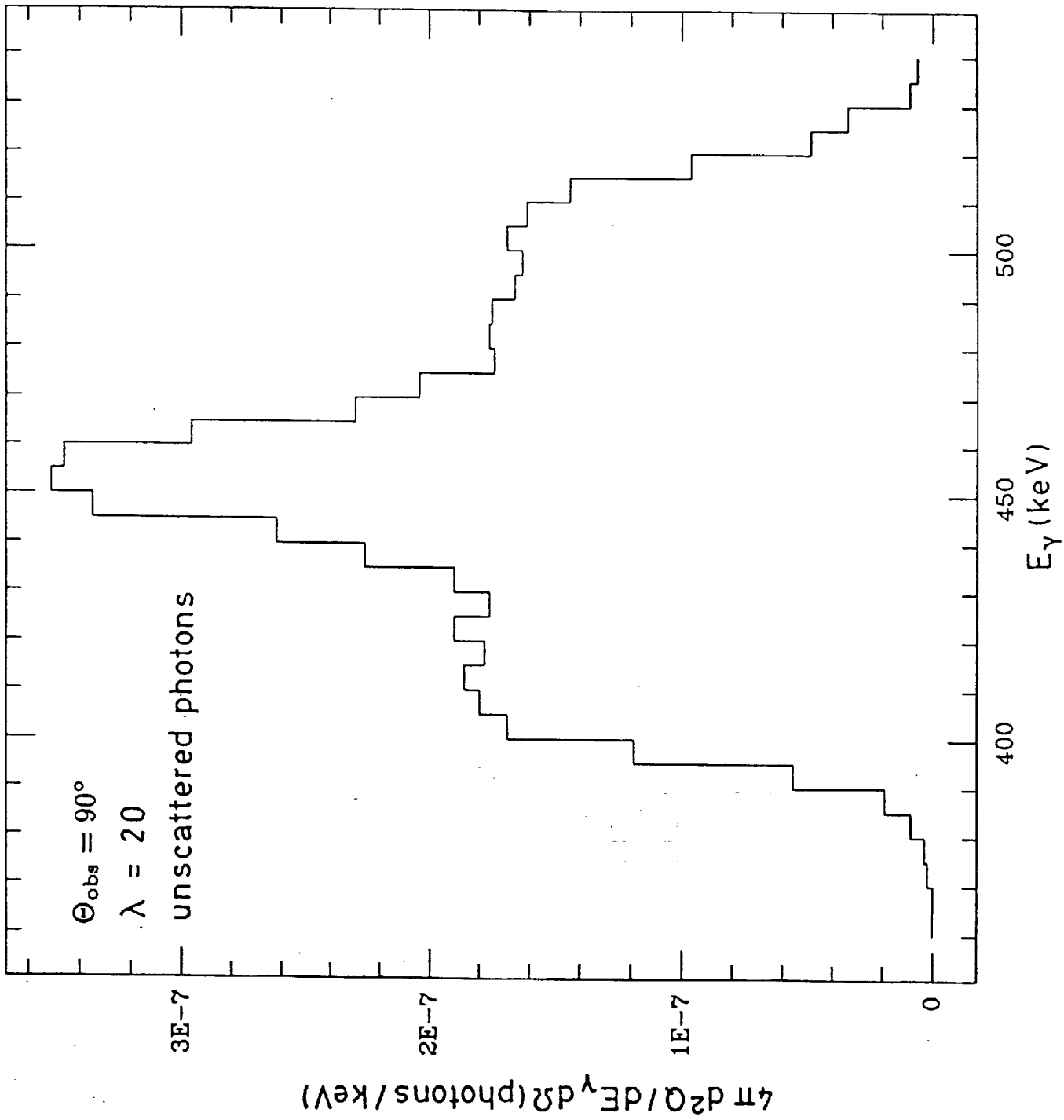

Figure 6

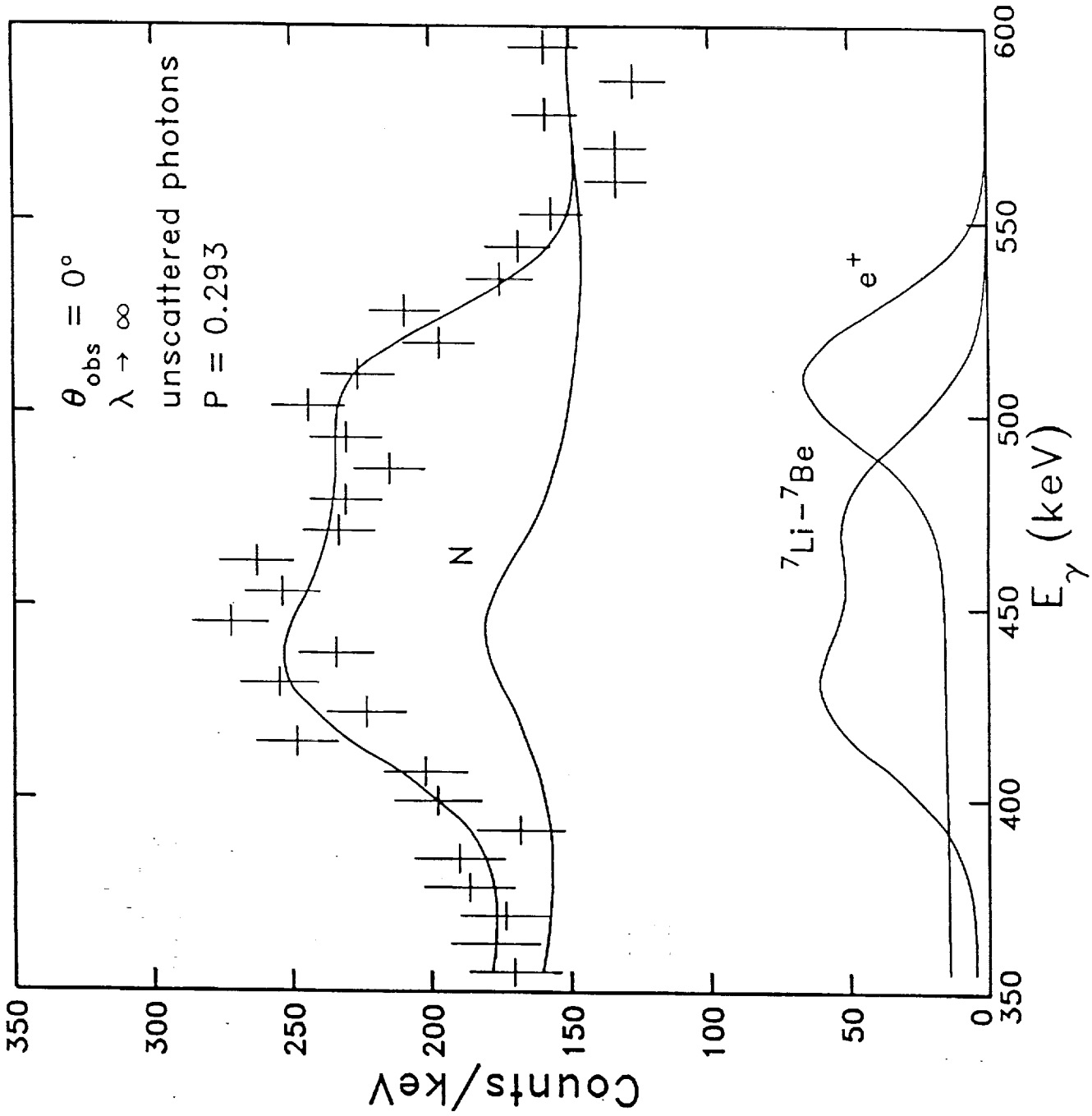

Figure 8

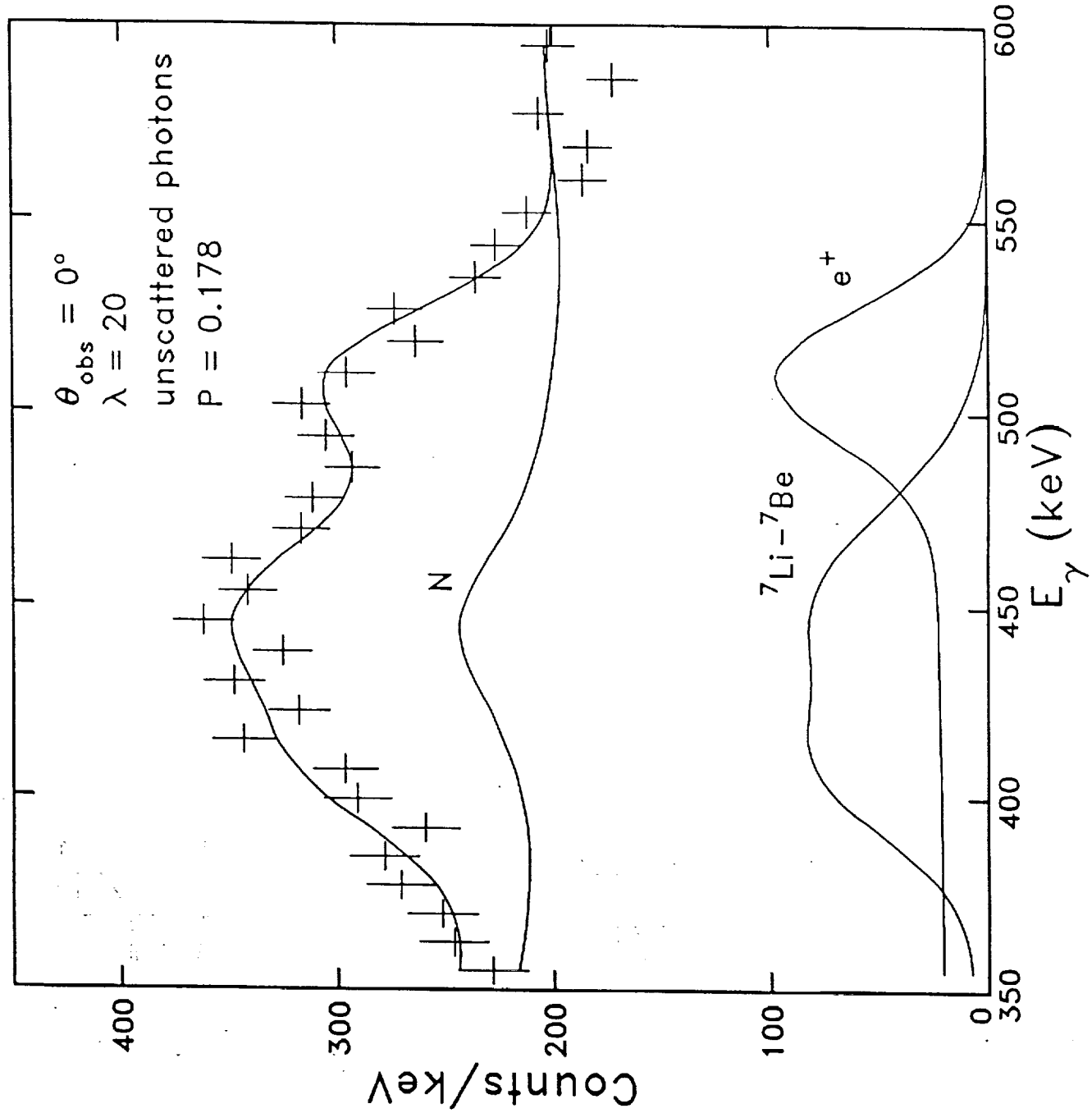

Figure 10

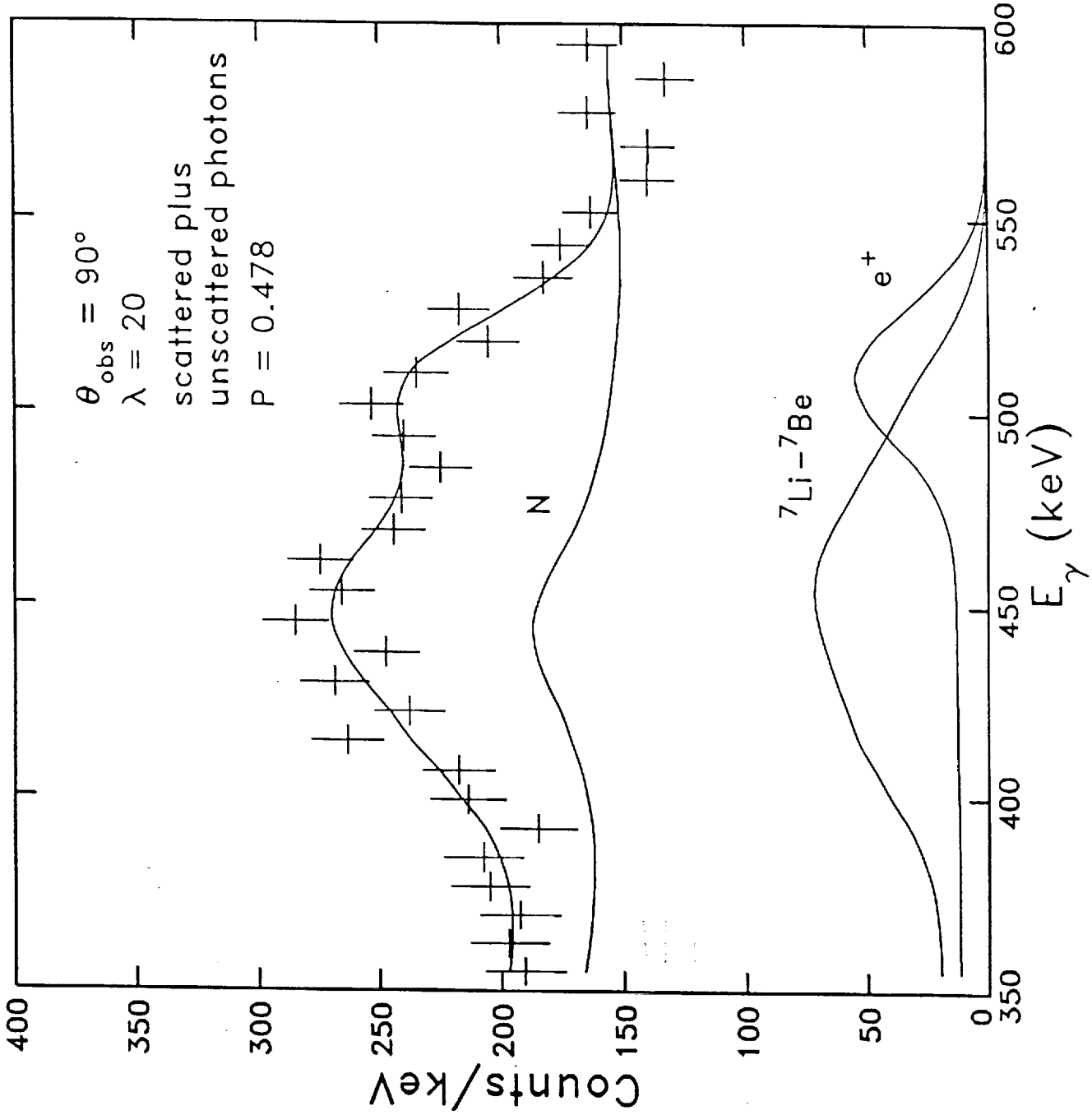

Figure 12

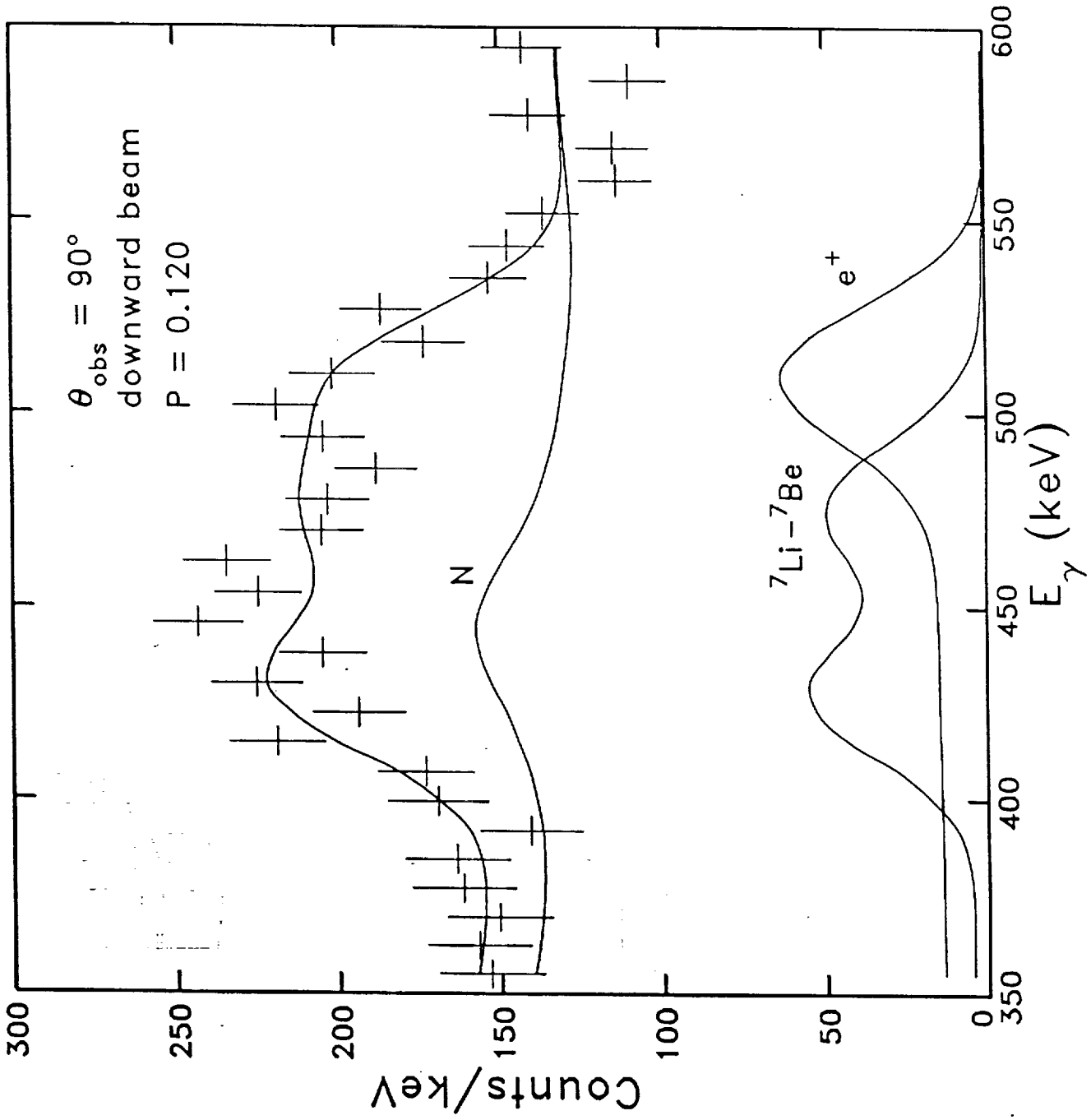

Figure 14

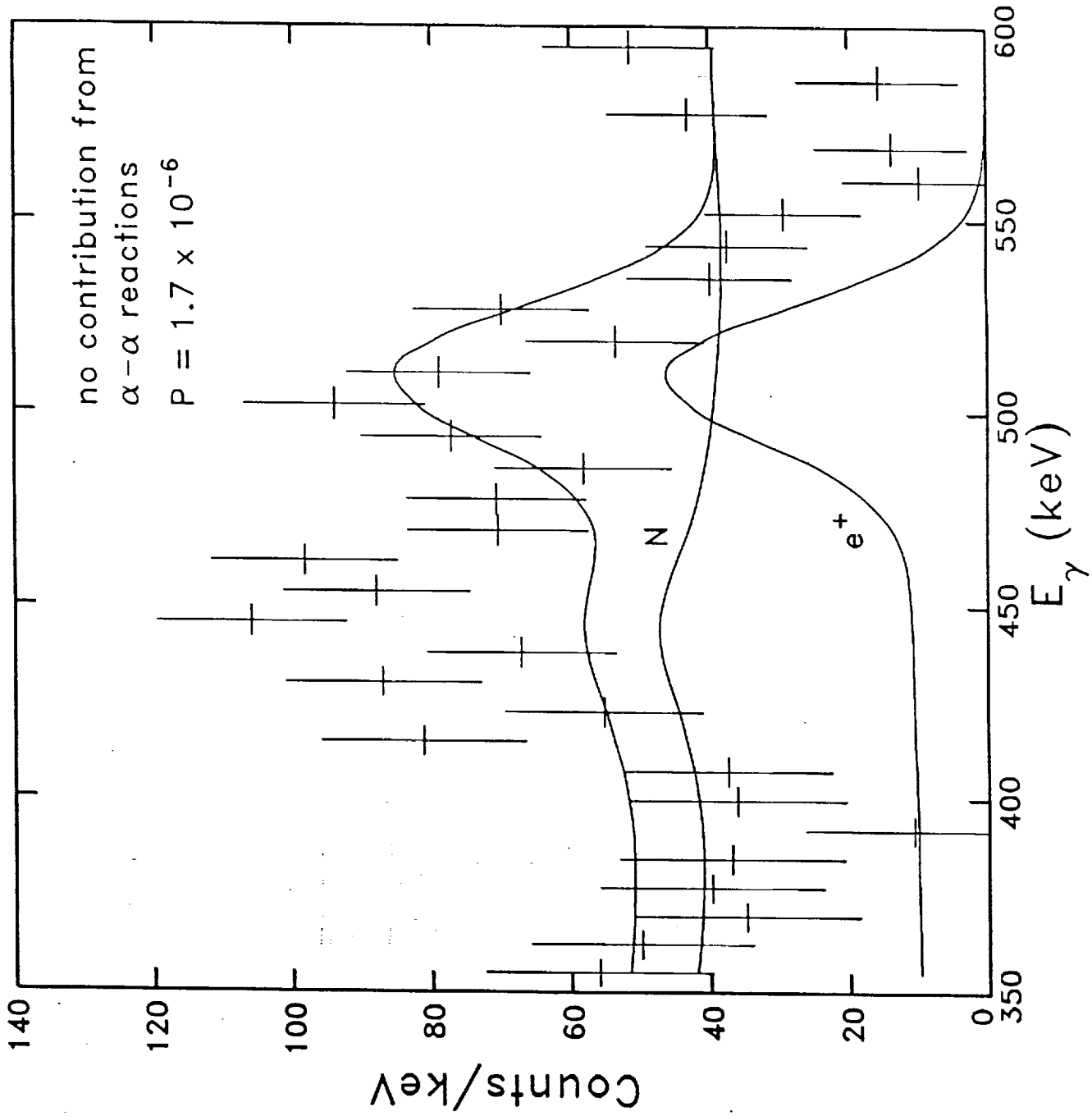

Figure 16

NASA
National Aeronautics and Space Administration

Report Documentation Page

1. Report No.	2. Government Accession No.	3. Recipient's Catalog No.

4. Title and Subtitle
Abundances from Solar-Flare Line Spectroscopy

5. Report Date
July 25, 1989

6. Performing Organization Code

7. Author(s)
Ronald J. Murphy

8. Performing Organization Report No.

10. Work Unit No.

9. Performing Organization Name and Address
Universities Space Research Association
Suite 212, American City Building
Columbia, MD 21044

11. Contract or Grant No.
NAS5-30534

13. Type of Report and Period Covered

12. Sponsoring Agency Name and Address
NASA Goddard Space Flight Center
Greenbelt, MD 20771

14. Sponsoring Agency Code

15. Supplementary Notes

16. Abstract

The work performed during the six month contract period is summarized. Most of this work was devoted to updating and improving the computer codes used the abundance analyses of solar-flare gamma-ray data. These modifications are itemized in detail. The abundance analysis technique was then applied to data obtained by the Gamma-Ray Spectrometer (GRS) of the Solar Maximum Mission (SMM) spacecraft for the 27 April 1981 solar flare to set constraints on the interacting-particle angular distribution. The results are presented in the final report.

17. Key Words (Suggested by Author(s))	18. Distribution Statement
Solar flare spectroscopy gamma-ray	

19. Security Classif. (of this report)	20. Security Classif. (of this page)	21. No. of pages	22. Price
		34	

NASA FORM 1626 OCT 86